Research Square

Preprints are preliminary reports that have not undergone peer review.
They should not be considered conclusive, used to inform clinical practice,
or referenced by the media as validated information.

Circularity, Capacity Breaches, and Import-Anchored EPR for Solar PV and Battery Waste: A Probabilistic MFA-LCA Framework Applied to Zimbabwe

Ndava Constantine Mupondo

mupondo69@gmail.com

National University of Science & Technology

Prayer Mupondo

National University of Science & Technology

Research Article

Keywords: circular economy, material flow analysis, solar PV waste, lithium-ion batteries, Extended Producer Responsibility

Posted Date: November 25th, 2026

DOI: https://doi.org/10.21203/rs.3.rs-11859324/v1

License: This work is licensed under a Creative Commons Attribution 4.0 International License.
Read Full License

Additional Declarations: No competing interests reported.

Circularity, Capacity Breaches, and Import-Anchored EPR for Solar PV and Battery Waste: A Probabilistic MFA-LCA Framework Applied to Zimbabwe

Ndava Constantine Mupondo[1,2*] and Prayer Mupondo[2,3†]

[1*]Statistics & Operations Research Department, National University of Science & Technology, Cnr Cecil Avenue & Gwanda Road, Bulawayo, Zimbabwe.

[2]Quantity Survey, National University of Science & Technology, Cnr Cecil Avenue & Gwanda Road, Bulawayo, Zimbabwe.

*Corresponding author(s). E-mail(s): mupondo69@gmail.com;
Contributing authors: mupondoprayer@gmail.com;
†These authors contributed equally to this work.

Abstract

Remarkably, rapid rollout of solar photovoltaic (PV) and lithium-ion battery energy storage systems (BESS) across import-dependent emerging economies, often accelerated by climate-induced hydropower shortfalls and ageing thermal fleets, generates any major delayed end-of-life (EoL) waste liability in jurisdictions lacking domestic manufacturing or recycling infrastructure, in many respects. To gauge capacity timing and energetic circularity, we formalize the regularized *Deferred Waste Liability Index* (**DWLI$_t$**) and the thermodynamically coherent *Circularity-Weighted Energy Return* (**CWER**), proving required and enough conditions for infrastructure lead times, net circular energy gains, and regional hub-and-spoke optimality, broadly speaking. A second generalizable estimation and policy-design framework is developed that integrates minimum-variance trade-and-survey triangulation, probabilistic dynamic material flow analysis (MFA), ISO 14040/14044 life cycle assessment (LCA), and regional scale-economy optimization, and verify it employing empirical data and three local operational case studies from Zimbabwe through 2060. In this

broader context, given zero existing formal PV or lithium-ion recycling capacity ($\mathbf{DWLI_t} \rightarrow +\infty$), even one capped 5,000 $\mathrm{t\,yr^{-1}}$ pilot trajectory is breaching the critical capacity threshold ($\mathbf{DWLI_t} > \mathbf{1}$) by 2042–2043 and peaks at **3.40** in 2050. Under the Accelerated Transition portfolio (13,415 MW PV and 7,813 MW/31,252 MWh BESS by 2040), cumulative EoL waste in Zimbabwe reaches 42,300 tonnes of PV and 28,400 tonnes of BESS by 2050, rising to 95,800 tonnes (95% prediction interval [PI]: 76,400–118,200) and 52,100 tonnes (95% PI: 41,200–64,900) by 2060; across all scenarios, combined cumulative waste spans 57,400–147,900 tonnes, with 76–81% of Accelerated Transition flows emerging between 2045 and 2060. Formal recovery is increasing **CWER** by 19.4% for PV (12.4 to 14.8) and 45.2% for BESS (4.2 to 6.1); by comparison, informal dismantling depresses net energy return (11.2 and 3.8) and augments carcinogenic human toxicity by factors of 3.2 and 8.7, respectively. An actuarially balanced import-anchored Extended Producer Responsibility (EPR) sinking-fund levy (USD 15–25 $\mathrm{kW^{-1}}$ for PV; USD 10.4–17.9 $\mathrm{kWh^{-1}}$ per battery cohort, or USD 19–33 $\mathrm{kWh^{-1}}$ over a 25-year PV-matched two-cycle horizon are derived) paired with informal-sector certification and Southern African Development Community (SADC) regional hydrometallurgical cooperation.

Keywords: circular economy; material flow analysis; solar PV waste; lithium-ion batteries; Extended Producer Responsibility

1 Introduction

While, accelerating decarbonization and grid resilience, this capital-import transition is creating an intertemporal governance paradox, including equipment installed to solve immediate power deficits is yielding a large, spatially scattered, and partially hazardous end-of-life (EoL) waste stream 10–25 years later, often in authorities with insignificant domestic hardware manufacturing, limited municipal waste budgets, and nascent formal recycling capacity [4, 25], in real-world scenarios. Against this backdrop, across sub-Saharan Africa and comparable import-dependent emerging economies, electricity supply expansion increasingly is counting on rapid rollout of crystalline silicon (c-Si) solar photovoltaics (PV) and lithium-ion battery energy storage systems (BESS) [12].

Without question, this structural dynamic is laid out by Zimbabwe. Total national installed generation capacity stands at nearly 2,962 MW, including 1,050 MW at the Kariba South hydropower station, 1,680 MW of ageing coal-fired thermal units, and 232 MW from small hydropower, bagasse and solar independent power producers (IPPs)—against peak demand exceeding 1,900 MW [26], in real-world scenarios. Zambezi River inflows have been curtailed by Recurrent El Niño-induced droughts, compressing Kariba South utilization below 32% during dry periods and lowering

trustworthy domestic generation to 1,200–1,600 MW [26], on the whole; to bridge this deficit, Zimbabwe's National Renewable Energy Policy (NREP) emphasized 1,100 MW of non-large-hydro renewables by 2025 and 2,100 MW by 2030 (incorporating 1,575 MW of solar PV), supported by duty-free importation of solar panels, inverters, and storage batteries [18].

Unlike standard municipal waste, retired PV modules and lithium-ion batteries are comprising regulated toxicants, remarkably guide in tin–lead (Sn–Pb) cell interconnects, trace cadmium in thin-film cohorts, cobalt, nickel and fluorinated lithium hexafluorophosphate ($LiPF_6$) electrolytes capable of hydrolysing into the hydrofluoric acid upon moisture or thermal exposure [8, 9, 22], in real-world scenarios. Under these conditions, nationally, Zimbabwe is creating roughly 17,000 tonnes of total electronic waste (e-waste) annually (1.1 $\mathrm{kg\,capita^{-1}}$), of which only 0.03 kt ($< 0.2\%$) is formally collected and recycled [2], with zero dedicated PV or lithium-ion battery processing plants [15], in actual application; under stochastic Mean-CVaR capacity expansion pathways projecting up to 13,415 MW of PV and 7,813 MW of BESS by 2040 [21, 26], initial batches commissioned during 2025–2030 will retire concurrently between 2040 and 2055 under the standard Weibull survival dynamics [23].

While it is true that dynamic and probabilistic material flow analysis (MFA) studies have quantified PV waste trajectories globally [11], in Mexico [7], and in Portugal [14], existing frameworks neither solve severe import-market data sparsity through the minimum-variance triangulation nor link dynamic waste flows to formal capacity lead-time bounds, thermodynamically uniform circular energy returns, and regional scale-economy thresholds. This study tackles three research questions:

RQ1. How can, by definition, theoretically thin trade, regulatory and field-survey datasets be integrated into a statistically defensible probabilistic MFA–LCA framework to project EoL solar PV and BESS stocks and hazardous inventories through 2060?

RQ2. At what temporal threshold do EoL waste flows primarily exceed attainable domestic treatment capacity, and what energetic and toxicological trade-offs originate across the formal recycling, informal dismantling, and sanitary landfilling?

RQ3. Most markedly, How can delayed EoL liabilities be actuarially internalized into the energy-planning models and controlled via an import-anchored Extended Producer Responsibility (EPR) and regional SADC mitigation architecture?

The paper contributes. Building on this observation, third, a thermodynamically coherent *Circularity-Weighted Energy Return* (CWER) are introduced, proving required and enough conditions under the which formal recovery increases, and informal dismantling degrades, net lifecycle energy return, and obtain an actuarial Weibull sinking-fund EPR charge and a regional hub-and-spoke optimality threshold, verifying the entire framework with Zimbabwean national data and three local operational case studies, on the whole. First a generalizable estimation pipeline is established combining Gauss–Markov minimum-variance inflow triangulation with Monte Carlo dynamic MFA and tailored ISO 14040/14044 LCA, and formalize the regularized *Deferred Waste Liability Index* (DWLI_t) and prove a closed-form policy lead-time bound, in actual application.

2 Literature Review and Theoretical Foundations

2.1 Dynamic and Probabilistic Material Flow Analysis under Data Sparsity

Physical stocks are being monitored by material flow analysis (MFA) and flows within this specified spatiotemporal boundaries, under the mass conservation [7], to a significant degree; Dynamic MFA is expanding static accounting by convolving annual capacity additions with stochastic lifetime distributions, ordinarily two-parameter Weibull curves encapsulating early infant-mortality failures, alongside wear-out retirement [17, 23], broadly speaking. Viewed through this lens, Monte Carlo simulation is embedded by recent advances to spread uncertainties in cohort mass intensity, survival shape, and collection rates, as showed for Portugal's decarbonization pathway [14] and multi-regional critical mineral exposure through 2050 [11].

Translating dynamic MFA to sub-Saharan Africa confronts acute data sparsity: unlike feed-in-tariff authorities with centralized registries, import-dependent markets lack broad inventories of distributed commercial and residential installations, in real-world scenarios; indeed, single-source estimates are biased by unrecorded cross-border trade and unpermitted installations, needing formal statistical reconciliation across the customs Harmonized System (HS) trade statistics, utility licensing registers, and organized installer surveys, in many respects.

2.2 Life Cycle Assessment of PV and Battery End-of-Life Pathways

Life cycle assessment (LCA) benchmarks environmental trade-offs across EoL management options [16]. Within this framework, for c-Si PV modules, pathways span uncontrolled dumping/open burning, sanitary landfilling, mechanical delamination (recovering bulk glass, aluminium frames, and copper), and thermal or chemical sharpening recovering solar-grade silicon and silver [4, 8, 10, 25], to a significant degree. For lithium-ion batteries, mostly nickel–manganese–cobalt (NMC) and lithium–iron–phosphate (LFP) chemistries, formal recycling includes pyrometallurgical smelting, hydrometallurgical leaching (hitting superior lithium and transition-metal recovery at lower process emissions), and emerging direct cathode regeneration [5, 9], to a significant degree.

The severity of unmanaged EoL disposal is disclosed by Empirical African LCA evidence; In Burkina Faso, Badza et al. [1] showed battery technology and EoL disposition dominate stand-alone PV life-cycle burdens, with formal recycling lowering lithium-ion battery impacts by 3–99%, across the impact categories relative to landfilling, to a significant degree. From this perspective, modifying global life-cycle inventories (e.g., ecoinvent) to Southern Africa needs adjusting upstream Chinese manufacturing mixes, maritime and inland freight corridors, domestic grid emission factors, and local informal emission profiles, where open burning and acid leaching organize heavy metals, dioxins, and fluorides into the soils and groundwater [19, 22], in many respects.

2.3 Extended Producer Responsibility and Informal Sector Integration

Circular economy policies are prioritizing value retention via repair, second-life repurposing, and high-efficiency material recovery [4, 10], in real-world scenarios; Extended Producer Responsibility (EPR) is implementing the polluter-pays principle by shifting physical and financial EoL obligations from municipalities to producers [25], in many respects. In light of this dynamic, regionally, South Africa's 2020 EPR Regulations under the National Environmental Management - Waste Act (NEMWA, Act No. 59 of 2008, Government Notice No. 1184) designate electrical and electronic equipment (EEE)—covering solar PV modules and batteries, for mandatory Producer Responsibility Organisation (PRO) membership, progressive recovery targets, and informal waste-picker integration [6].

Directly transplanting manufacturer-centric EPR into the wholly import-dependent economies faces institutional restrictions: hardware enters almost fully via fragmented importers and distributors, weakening post-market enforcement, in many respects; during this period, urban scrap recovery is dominated by informal collectors, and as Wilson et al. [24] establish, excluding informal recyclers depresses capture rates and harms livelihoods, in real-world scenarios. In parallel with this, by comparison, formalization via cooperatives, occupational certification, and guaranteed off-take tariffs is raising both recovery efficiency and social equity [15, 19].

2.4 Energy Return Metrics and Deferred Liabilities

Lifetime electricity is appraised by Standard Energy Return on Investment (EROI) delivered relative to cumulative embodied energy [20], with Energy Stored on Invested (ESOI) broadening the metric to storage assets [3], broadly speaking. Standard expressions, still, exclude EoL material recovery credits and environmental remediation burdens. Also prior circularity adjustments that add recovered energy solely to the numerator suffer a logical defect: under the destructive informal dismantling, non-negative numerator adjustments can't represent net energy degradation, in many respects. Correspondingly, standard MFA tonnage outputs omit formal benchmarking against time-varying domestic treatment capacity.

3 Generalizable Estimation Framework and Formal Analysis

Figure 1 reveals the integrated estimation pipeline linking statistical inflow triangulation, Monte Carlo dynamic MFA, ISO 14040/14044 LCA, diagnostic indices (DWLI_t, CWER), and actuarial EPR and regional mitigation optimization, broadly speaking; full posterior/empirical uncertainty is being passed by each individual stage bounds forward so that policy thresholds reflect joint statistical and technological, with a center on economic uncertainty, to a significant degree.

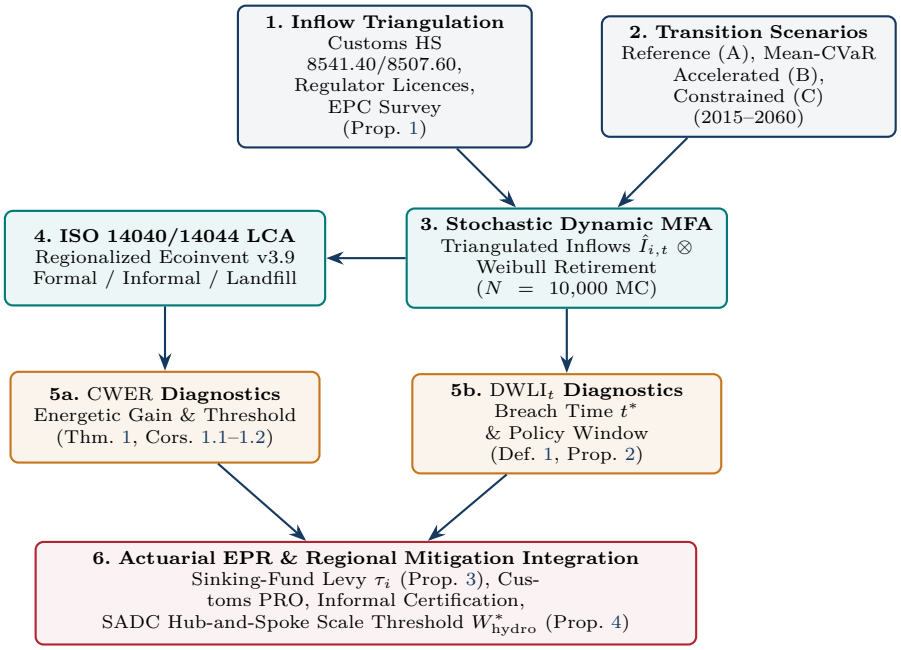


Fig. 1: Coherent estimation and policy-design architecture coupling minimum-variance inflow triangulation, probabilistic dynamic MFA, ISO LCA, circularity diagnostics, and regional mitigation optimization.

3.1 Minimum-Variance Inflow Triangulation and Dynamic MFA

Let $i \in \{\text{PV}, \text{BESS}\}$ index the hardware stream. Customs trade logs capture aggregate mass across utility, commercial/industrial (C&I), and residential segments subject to informal cross-border leakage $\rho_{i,t} \in [0, 1)$, whereas regulatory registries capture only licensed installations and field surveys exhibit sampling variance. For historical year $t \in [t_0, t_{\text{curr}}]$, let $I^{\text{cust}}_{i,t} = (1 - \rho_{i,t})\, M^{\text{imp}}_{i,t} / \mu_{i,t}$ signify leakage-adjusted customs capacity (where $M^{\text{imp}}_{i,t}$ is net imported mass and $\mu_{i,t}$ is group mass intensity in $\text{t}\,\text{MW}^{-1}$ or $\text{t}\,\text{MWh}^{-1}$), and let $I^{\text{surv}}_{i,t}$ designate the resolved bottom-up registry-plus-survey capacity estimator, in real-world scenarios.

Proposition 1 (Minimum-Variance Triangulation and Uncertainty Propagation)**.** *Suppose $I^{\text{cust}}_{i,t}$ and $I^{\text{surv}}_{i,t}$ are autonomous unbiased estimators of true annual capacity addition $I_{i,t}$ with finite variances $\sigma^2_{\text{cust},i,t} > 0$ and $\sigma^2_{\text{surv},i,t} > 0$, to a significant degree; among all affine unbiased estimators $\tilde{I}_{i,t}(\omega) = \omega\, I^{\text{cust}}_{i,t} + (1 - \omega)\, I^{\text{surv}}_{i,t}$ hypothetically,*

the unique minimum-variance (Gauss–Markov) estimator is

$$\hat{I}_{i,t} = w_{i,t}\, I^{\text{cust}}_{i,t} + (1 - w_{i,t})\, I^{\text{surv}}_{i,t}, \qquad w_{i,t} = \frac{\sigma^2_{\text{surv},i,t}}{\sigma^2_{\text{cust},i,t} + \sigma^2_{\text{surv},i,t}}, \tag{1}$$

with strictly reduced estimator variance

$$\text{Var}(\hat{I}_{i,t}) = \left(\sigma^{-2}_{\text{cust},i,t} + \sigma^{-2}_{\text{surv},i,t}\right)^{-1} < \min\left(\sigma^2_{\text{cust},i,t},\ \sigma^2_{\text{surv},i,t}\right). \tag{2}$$

Proof Unbiasedness is holding identically, because $\mathbb{E}[\tilde{I}_{i,t}(\omega)] = \omega I_{i,t} + (1-\omega) I_{i,t} = I_{i,t}$ for all $\omega \in \mathbb{R}$; replacing $w_{i,t}$ into $g(\omega^*)$ creates $\frac{\sigma^2_{\text{cust},i,t}\sigma^2_{\text{surv},i,t}}{\sigma^2_{\text{cust},i,t}+\sigma^2_{\text{surv},i,t}} = (\sigma^{-2}_{\text{cust},i,t} + \sigma^{-2}_{\text{surv},i,t})^{-1}$, which is strictly smaller than either constituent variance, because both precisions $\sigma^{-2}_{\text{cust},i,t}, \sigma^{-2}_{\text{surv},i,t}$ are strictly positive, on the whole. Differentiating yields $g'(\omega) = 2\omega\sigma^2_{\text{cust},i,t} - 2(1-\omega)\sigma^2_{\text{surv},i,t} = 0$ and $g''(\omega) = 2(\sigma^2_{\text{cust},i,t} + \sigma^2_{\text{surv},i,t}) > 0$, starting the unique global minimizer $\omega^* = w_{i,t}$ in (1). Taken together, independence is giving $g(\omega)\text{Var}(\tilde{I}_{i,t}(\omega)) = \omega^2\sigma^2_{\text{cust},i,t} + (1-\omega)^2\sigma^2_{\text{surv},i,t}$. □

Annual EoL waste flow $\dot{W}_{i,t}$ ($\text{t}\,\text{yr}^{-1}$) and cumulative waste $W_{i,T}$ (t) are acquired by discrete convolution of historical ($\hat{I}_{i,\tau}$) and scenario-projected inflows with a two-parameter Weibull retirement probability mass function:

$$\dot{W}_{i,t} = \sum_{\tau=t_0}^{t} \mu_{i,\tau}\, I_{i,\tau}\, [F_i(t-\tau+1;\alpha_i,\beta_i) - F_i(t-\tau;\alpha_i,\beta_i)], \qquad W_{i,T} = \sum_{t=t_0}^{T} \dot{W}_{i,t}, \tag{3}$$

where $F_i(\Delta;\alpha_i,\beta_i) = 1 - \exp(-(\Delta/\beta_i)^{\alpha_i})$ for $\Delta \geq 0$, with shape $\alpha_i > 1$ and scale $\beta_i = \bar{L}_i/\Gamma(1 + 1/\alpha_i)$. Along these dimensions, to uphold statistical coherence across all downstream modules, $N = 10{,}000$ joint Monte Carlo draws over $(\alpha_i, \beta_i, \mu_{i,\tau}, \rho_{i,\tau}, I_{i,\tau})$—sampling historical inflows from $\mathcal{N}(\hat{I}_{i,\tau}, \text{Var}(\hat{I}_{i,\tau}))$ shortened at zero, yield empirical medians and 95% prediction intervals (PIs) for $\dot{W}_{i,t}$, which are feeding directly into LCA impact inventories and capacity-deficit calculations, on the whole.

3.2 Regularized Deferred Waste Liability Index (DWLI_t)

A capacity-benchmarked dynamic indicator is formalized. Against this backdrop, static MFA tonnage forecasts do not disclose when waste generation overwhelms domestic processing capacity, in many respects.

Definition 1 (Deferred Waste Liability Index and Preparedness Deficit)**.** Let $\dot{W}_{i,t} \geq 0$ signify annual EoL waste for stream i in year t, $C_{i,t} \geq 0$ the installed domestic or contracted regional recycling capacity, and $\phi_i \in (0, 1]$ the attainable formal collection and recovery efficiency, to a significant degree; the regularized *Deferred Waste Liability Index* is specified as

$$\mathrm{DWLI}_t(\epsilon) = \frac{\sum_i \dot{W}_{i,t}}{\sum_i C_{i,t}\,\phi_i + \epsilon}, \qquad \epsilon > 0, \tag{4}$$

with limit $\mathrm{DWLI}_t \lim_{\epsilon \to 0^+} \mathrm{DWLI}_t(\epsilon) \in [0, \infty]$ (taking $+\infty$ whenever $\sum_i \dot{W}_{i,t} > 0$ and $\sum_i C_{i,t}\phi_i = 0$), which is why over planning horizon $[t_0, T]$, the *Cumulative Preparedness Deficit* (tonnes) is

$$\mathcal{D}_T = \int_{t_0}^{T} \max\left(0,\ \sum_i \dot{W}_{i,t} - \sum_i C_{i,t}\,\phi_i\right) dt. \tag{5}$$

Effective treatment capacity is exceeded by annual retirements, forcing excess waste into the stockpiling, informal dismantling, or landfilling, whenever $\mathrm{DWLI}_t > 1$, to a significant degree.

Proposition 2 (Capacity-Breach Time and Maximum Policy Lead-Time Bound)**.** *Suppose combined annual waste flow $\dot{W}(t) \sum_i \dot{W}_{i,t}$ is strictly increasing on $[t_0, t_{\mathrm{peak}}]$. Also, effective treatment capacity expands linearly from plant commissioning $t_{\mathrm{comm}} > t_0$ at ramp rate $\kappa > 0$, i.e., $\Phi(t) \sum_i C_{i,t}\phi_i = \kappa\,(t - t_{\mathrm{comm}})_+$. Let $\Delta_{\mathrm{inst}} = t_{\mathrm{comm}} - t_{\mathrm{pol}}$ represent the institutional-to-commissioning direct time from policy enactment t_{pol}. Then:*

(a) An initial capacity breach ($\mathrm{DWLI}_t = +\infty > 1$) is principally guaranteed on $[t_0, t_{\mathrm{comm}}]$ whenever $\dot{W}(t) > 0$, accumulating preparedness deficit $\mathcal{D}_{t_{\mathrm{comm}}} = \int_{t_0}^{t_{\mathrm{comm}}} \dot{W}(t)\,dt > 0$, in real-world scenarios.

(b) Avoiding a mid-horizon structural breach ($\mathrm{DWLI}_{t_{\mathrm{peak}}} \leq 1$) at peak year $t_{\mathrm{peak}} > t_{\mathrm{comm}}$ is, to a large extent, needing

$$t_{\mathrm{pol}} \leq t_{\mathrm{peak}} - \frac{\dot{W}(t_{\mathrm{peak}})}{\kappa} - \Delta_{\mathrm{inst}}. \tag{6}$$

Proof For (a), on $t \in [t_0, t_{\mathrm{comm}}]$, $(t - t_{\mathrm{comm}})_+ = 0$ is suggesting $\Phi(t) = 0$; indeed, rearranging gives $t_{\mathrm{comm}} \leq t_{\mathrm{peak}} - \dot{W}(t_{\mathrm{peak}})/\kappa$, and replacing $t_{\mathrm{comm}} = t_{\mathrm{pol}} + \Delta_{\mathrm{inst}}$ proves (6); in turn,

by Definition 1, $\dot{W}(t) > 0$ is yielding $\mathrm{DWLI}_t = +\infty > 1$ and $\max(0, \dot{W}(t) - \Phi(t)) = \dot{W}(t)$, so $\mathcal{D}_{t_{\mathrm{comm}}} = \int_{t_0}^{t_{\mathrm{comm}}} \dot{W}(t)\, dt > 0$, on the whole. Viewed through this lens, for (b), non-exceedance at t_{peak} is needing $\mathrm{DWLI}_{t_{\mathrm{peak}}} \leq 1 \iff \dot{W}(t_{\mathrm{peak}}) \leq \Phi(t_{\mathrm{peak}}) = \kappa(t_{\mathrm{peak}} - t_{\mathrm{comm}})$. □

Corollary 2.1 (Critical Policy Window for Zimbabwe)**.** *Under Scenario B, combined annual retirements in Zimbabwe are reaching* $\dot{W}(2050) \approx 11{,}900\ t\,yr^{-1}$ *(median; 95% PI upper bound* $\approx 14{,}700\ t\,yr^{-1}$*), needing* 17,000–21,000 $t\,yr^{-1}$ *of nameplate capacity at* $\phi = 0.70$ *(rising to* 25,000–30,000 $t\,yr^{-1}$ *with a 20–40% surge buffer), in real-world scenarios. From this perspective, with an effective capacity ramp rate* $\kappa \approx 1{,}400\ t\,yr^{-2}$ *and an institutional-to-commissioning lag* $\Delta_{\mathrm{inst}} \in [11, 14]$ *years (incorporating legislation, PRO formation, financing and construction),* $t_{\mathrm{pol}} \leq 2050 - 8.5 - \Delta_{\mathrm{inst}} \in [2027.5, 2030.5]$ *are produced by (6), on the whole. Passing binding EPR policy after 2030 mathematically precludes avoiding a 2042–2050 capacity deficit.*

3.3 Thermodynamically Consistent Circularity-Weighted Energy Return (CWER)

Prior circularity metrics that add recovered material energy solely to the numerator of EROI_0 omit EoL processing energy and environmental remediation burdens, creating a formal inconsistency whereby CWER can never drop below EROI_0 even under the destructive informal dismantling; this flaw below is tackled, on the whole.

Definition 2 (Circularity-Weighted Energy Return)**.** For a technology cohort with lifetime electricity output E_{out}, manufacturing and balance-of-system embodied energy $E_{\mathrm{in}} > 0$, and baseline linear energy return $\mathrm{EROI}_0 E_{\mathrm{out}}/E_{\mathrm{in}}$, let $\boldsymbol{\eta} = (\eta_1, \ldots, \eta_M) \in [0,1]^M$ signify material recovery efficiencies across EoL constituents $m \in \{1, \ldots, M\}$ of mass M_m^{EoL} and primary embodied energy $e_m > 0$. Let $E_{\mathrm{EoL}}(\boldsymbol{\eta}) \geq 0$ represent EoL collection, transport, and recycling energy. Also, $E_{\mathrm{rem}}(\boldsymbol{\eta}) \geq 0$ designate the energy equivalent of environmental remediation and unrecovered hazardous-waste externalities. Then:

$$\mathrm{CWER}(\boldsymbol{\eta}) = \frac{E_{\mathrm{out}} + \sum_{m=1}^{M} M_m^{\mathrm{EoL}}\, e_m\, \eta_m}{E_{\mathrm{in}} + E_{\mathrm{EoL}}(\boldsymbol{\eta}) + E_{\mathrm{rem}}(\boldsymbol{\eta})}. \tag{7}$$

Theorem 1 (Necessary and Sufficient Condition for Circular Energy Gain)**.** *Under Definition 2, a circular EoL pathway strictly is boosting net system energy return*

($\mathrm{CWER}(\boldsymbol{\eta}) > \mathrm{EROI}_0$*) if and only if*

$$\sum_{m=1}^{M} M_m^{\mathrm{EoL}}\, e_m\, \eta_m > \mathrm{EROI}_0 \left[E_{\mathrm{EoL}}(\boldsymbol{\eta}) + E_{\mathrm{rem}}(\boldsymbol{\eta})\right], \tag{8}$$

or equivalently, whenever $E_{\mathrm{EoL}}(\boldsymbol{\eta}) + E_{\mathrm{rem}}(\boldsymbol{\eta}) > 0$*, the insignificant circular energy return fulfills* $\mathrm{EROI}_{\mathrm{EoL}}(\boldsymbol{\eta}) \frac{\sum_m M_m^{\mathrm{EoL}} e_m \eta_m}{E_{\mathrm{EoL}}(\boldsymbol{\eta}) + E_{\mathrm{rem}}(\boldsymbol{\eta})} > \mathrm{EROI}_0$*.*

Proof Since $E_{\mathrm{in}} > 0$ and $E_{\mathrm{EoL}}(\boldsymbol{\eta}) + E_{\mathrm{rem}}(\boldsymbol{\eta}) \geq 0$, the denominator of (7) is, in effect, strictly positive; in turn, multiplying both sides of $\mathrm{CWER}(\boldsymbol{\eta}) > E_{\mathrm{out}}/E_{\mathrm{in}}$ by $E_{\mathrm{in}}\left[E_{\mathrm{in}} + E_{\mathrm{EoL}}(\boldsymbol{\eta}) + E_{\mathrm{rem}}(\boldsymbol{\eta})\right] > 0$ gives

$$E_{\mathrm{in}}E_{\mathrm{out}} + E_{\mathrm{in}} \sum_{m=1}^{M} M_m^{\mathrm{EoL}} e_m \eta_m > E_{\mathrm{in}}E_{\mathrm{out}} + E_{\mathrm{out}}\left[E_{\mathrm{EoL}}(\boldsymbol{\eta}) + E_{\mathrm{rem}}(\boldsymbol{\eta})\right], \textit{broadly speaking.}$$

Dividing by $E_{\mathrm{EoL}}(\boldsymbol{\eta}) + E_{\mathrm{rem}}(\boldsymbol{\eta}) > 0$ is generating the equal $\mathrm{EROI}_{\mathrm{EoL}}$ bound, so cancelling $E_{\mathrm{in}}E_{\mathrm{out}}$ and dividing by $E_{\mathrm{in}} > 0$ yields (8), broadly speaking. □

Corollary 1.1 (Informal-Sector Energy Penalty)**.** *Under informal dismantling (*$\boldsymbol{\eta}_{\mathrm{inf}}$*), high-embodied-energy constituents (solar-grade silicon, silver, lithium, cobalt, and sharpened graphite) remain unrecovered (*$\eta_m \approx 0$ *except bulk aluminium/copper scrap), in real-world scenarios; theorem 1 guarantees* $\mathrm{CWER}(\boldsymbol{\eta}_{\mathrm{inf}}) < \mathrm{EROI}_0$*, whenever* $\sum_m M_m^{\mathrm{EoL}} e_m \eta_{m,\mathrm{inf}} < \mathrm{EROI}_0[E_{\mathrm{EoL}}(\boldsymbol{\eta}_{\mathrm{inf}}) + E_{\mathrm{rem}}(\boldsymbol{\eta}_{\mathrm{inf}})]$*. From this perspective, simultaneously, open burning and soil/groundwater contamination impose major remediation burdens* $E_{\mathrm{rem}}(\boldsymbol{\eta}_{\mathrm{inf}}) > 0$*.*

Corollary 1.2 (Minimum Weighted Recovery Efficiency for Energetic Viability)**.** *Let* $E_{\mathrm{mat}}^{\mathrm{tot}} \sum_{m=1}^{M} M_m^{\mathrm{EoL}} e_m$ *signify total primary embodied energy of the retired hardware and* $\bar{\eta} \frac{1}{E_{\mathrm{mat}}^{\mathrm{tot}}} \sum_{m=1}^{M} M_m^{\mathrm{EoL}} e_m \eta_m$ *the energy-weighted accumulate recovery efficiency, to a significant degree; indeed, a formal recycling plant hits net energy gain (*$\mathrm{CWER} > \mathrm{EROI}_0$*) if and only if*

$$\bar{\eta} > \bar{\eta}_{\mathrm{min}} \frac{\mathrm{EROI}_0\left[E_{\mathrm{EoL}}(\boldsymbol{\eta}) + E_{\mathrm{rem}}(\boldsymbol{\eta})\right]}{E_{\mathrm{mat}}^{\mathrm{tot}}}. \tag{9}$$

Proof Replacing $\sum_m M_m^{\mathrm{EoL}} e_m \eta_m = \bar{\eta}\, E_{\mathrm{mat}}^{\mathrm{tot}}$ into (8) and dividing by $E_{\mathrm{mat}}^{\mathrm{tot}} > 0$ produces (9) directly. □

3.4 Actuarial EPR Sinking-Fund Charge and Regional Mitigation Optimality

To internalize EoL liabilities into the capacity expansion models and appraise national versus regional recycling investments evidently, two closed-form economic conditions are devised, in real-world scenarios.

Proposition 3 (Actuarial EPR Sinking-Fund Levy under Stochastic Retirement)**.** *Let c_i^{EoL} represent the real net unit EoL treatment and reverse-logistics cost per tonne of technology i (net of secondary material revenues) at target recovery rate ϕ_i^{target}, and let $f_i(u)$ be the Weibull retirement probability density for cohort age $u \geq 0$, on the whole. Under a continuous real fund discount rate $r > 0$, the actuarially fair upfront levy τ_i (USD MW^{-1} or USD MWh^{-1}) collected at import/installation is*

$$\tau_i = \mu_i \, c_i^{\mathrm{EoL}} \, \phi_i^{\mathrm{target}} \int_0^{\infty} e^{-ru} f_i(u) \, du = \mu_i \, c_i^{\mathrm{EoL}} \, \phi_i^{\mathrm{target}} \, \mathcal{L}\{f_i\}(r), \tag{10}$$

where $\mathcal{L}\{f_i\}(r)$ is the Laplace transform of f_i.

Proof One installed unit of technology i embeds mass μ_i, of which fraction ϕ_i^{target} is formally recovered, across the retirement ages $u \in [0, \infty)$ with probability density $f_i(u)$, in actual application, and discounting expected instantaneous EoL expenditure $\mu_i c_i^{\mathrm{EoL}} \phi_i^{\mathrm{target}} f_i(u) \, du$ back to installation ($u = 0$) at real rate r and blending over $[0, \infty)$ gives (10), and this ensures projected discounted fund reserves equal expected EoL obligations, on the whole. □

Proposition 4 (Regional Hub-and-Spoke Scale Threshold)**.** *Consider an import-dependent country making W tonnes yr^{-1} of retired BESS packs. Let domestic full hydrometallurgical refining incur annualized fixed capital cost K_{dom} and unit operating cost v_{dom}; whereas a regional hub-and-spoke approach, spanning domestic discharging, dismantling and black-mass concentration at annualized fixed cost $K_{\mathrm{pre}} < K_{\mathrm{dom}}$ and unit cost v_{pre}, followed by export of black-mass fraction $\theta \in (0, 1)$ at cross-border transport cost c_{trans} and regional refining gate fee v_{reg}—satisfies $v_{\mathrm{pre}} + \theta(c_{\mathrm{trans}} + v_{\mathrm{reg}}) > v_{\mathrm{dom}}$, in actual application. Then total annualized mitigation cost is strictly minimized if and only by the regional hub-and-spoke approach if*

$$W < W^*_{\mathrm{hydro}} \frac{K_{\mathrm{dom}} - K_{\mathrm{pre}}}{v_{\mathrm{pre}} + \theta(c_{\mathrm{trans}} + v_{\mathrm{reg}}) - v_{\mathrm{dom}}}. \tag{11}$$

Proof Total annualized costs are widely $\mathrm{TC}_{\mathrm{dom}}(W) = K_{\mathrm{dom}} + v_{\mathrm{dom}}W$ and $\mathrm{TC}_{\mathrm{reg}}(W) = K_{\mathrm{pre}} + [v_{\mathrm{pre}} + \theta(c_{\mathrm{trans}} + v_{\mathrm{reg}})]W$. Taken together, strict dominance $\mathrm{TC}_{\mathrm{reg}}(W) < \mathrm{TC}_{\mathrm{dom}}(W)$ is equal to $[v_{\mathrm{pre}} + \theta(c_{\mathrm{trans}} + v_{\mathrm{reg}}) - v_{\mathrm{dom}}]W < K_{\mathrm{dom}} - K_{\mathrm{pre}}$, which is generating (11) upon dividing by the positive slight cost differential, in many respects. □

4 Empirical Validation Data, Scenarios, and LCA Specification

4.1 System Boundary and Zimbabwean Inflow Triangulation

Within national borders, the validation scope spans 2015 (the onset of commercial-scale solar imports in Zimbabwe) to 2060, in real-world scenarios. Lead-acid batteries are excluded from the primary MFA balance, because they are exhibiting separate electrochemistry, shorter lifespans (3–5 years), and entrenched, albeit chiefly informal, scrap smelting channels, in real-world scenarios. The LCA boundary encompasses upstream extraction and cell/module manufacturing (mostly Chinese supply chains), maritime freight to Beira and Durban ports, inland rail/road transport, and domestic EoL processing. In this broader context, product scope is covering utility-scale IPPs, C&I installations, and distributed solar home systems (SHS) applying c-Si PV modules (QLATEXz0000q of Zimbabwean imports, with QLATEXz0001q CdTe thin-film) and lithium-ion BESS (NMC and LFP chemistries).

Historical capacity additions (2015–2025) were triangulated via Equation (1) from three autonomous datasets: (i) Zimbabwe Revenue Authority (ZIMRA) customs records under HS 8541.40 (PV cells/modules) and HS 8507.60 (lithium-ion accumulators), audited for re-export and informal cross-border leakage $\rho_{i,t} \in [0.05, 0.12]$; (ii) ZERA IPP licences and net-metering registers (2018–2025); and (iii) ordered surveys of solar engineering, procurement, and construction (EPC) firms in Harare and Bulawayo ($n = 47$), in actual application. Cross-validation benchmarked implied per-capita additions against regional SADC peers. Table 1 recapitulates the stochastic MFA parameters obtained from Weckend et al. [23], IRENA [13], Harper et al. [9], Raugei et al. [20], Barnhart & Benson [3], and domestic EPC audits, on the whole.

4.2 Energy-Transition Scenarios (2015–2060)

Three cases spanning Zimbabwe's 2040 planning horizon and expanded through 2060 as replacement-stabilized regimes represent structural deployment uncertainty without forcing subjective scenario probabilities:

Table 1: Stochastic Material Flow Analysis Parameters and Uncertainty Priors

Parameter	PV Modules (c-Si)	Lith
Mean lifetime $\bar{L}_i$ (yr)	25.0 (SD: 3.0)	Util
Weibull shape α_i	2.5 (range: 2.1–3.2)	
Mass intensity $\mu_{i,2025}$	62 t MW^{-1} (55–70)	
Material shares (%)	Glass 70.0; Al 18.0; Polymers 6.0; Si 3.5; Cu 1.5; Trace 1.0	Cathode 27.0; Casing 20.0;
Baseline EROI_0 / ESOI_0	12.4	
Customs leakage $\rho_{i,t}$	0.08 (0.05–0.12)	

Scenario A: Reference Deployment (RD).

Extrapolates historical import growth and ZERA licensing pipelines: PV expands from 500 MW (2025) to 8,000 MW (2040) and stabilizes at 12,000 MW by 2050; BESS is reaching 4,000 MW (16,000 MWh at 4 h duration) by 2040, broadly speaking.

Scenario B: Accelerated Transition (AT).

Aligns with a stochastic Mean-CVaR best capacity expansion portfolio [21, 26], reaching 13,415 MW of PV and 7,813 MW (31,252 MWh) of BESS by 2040, and maturing at 18,500 MW PV and 10,800 MW (43,200 MWh) BESS by 2050, in real-world scenarios.

Scenario C: Constrained Growth (CG).

Reflects protracted macroeconomic financing bottlenecks, delayed grid reinforcement, and continued coal reliance, capping 2040 capacity at 5,000 MW PV and 1,500 MW (6,000 MWh) BESS, broadly speaking.

4.3 ISO 14040/14044 Life Cycle Assessment Adaptation

Life cycle impacts are modelled per tonne of retired hardware following ISO 14040/14044 applying ecoinvent v3.9 accommodated for Chinese manufacturing electricity mixes, maritime and Beira/Durban corridor transport, and Zimbabwean grid emission factors [1, 16, 22], in real-world scenarios. Three EoL management pathways are assessed: (1) *formal recycling* (70% target recovery via mechanical PV delamination and hydrometallurgical battery leaching); (2) *informal dismantling* (manual stripping of aluminium frames and copper cables combined with open burning of encapsulants and uncontrolled electrolyte dumping); and (3) *sanitary landfilling* (engineered containment without secondary material recovery), to a significant degree. Taken together, impact categories include climate change (kg CO_2-eq), carcinogenic

and non-carcinogenic human toxicity (CTUh), freshwater ecotoxicity (CTUe), and abiotic mineral resource depletion (kg Sb-eq).

5 Empirical Results, Local Case Studies, and Robustness

5.1 Projected National Waste Volumes and Material Stocks

Table 2 and cumulative EoL waste trajectories are provided from 2035 to 2060 by Figure 2. Under Scenario B (AT), cumulative PV waste rises from 1,800 tonnes in 2035 to 42,300 tonnes in 2050 and 95,800 tonnes (95% PI: 76,400–118,200) by 2060, in many respects. Owing to shorter electrochemical lifespans (9–12 years versus 25 years for PV), BESS waste accumulates more swiftly in relative terms, reaching 28,400 tonnes by 2050 and 52,100 tonnes (95% PI: 41,200–64,900) by 2060, in real-world scenarios. From this perspective, across all situations, combined 2060 cumulative waste spans 57,400 tonnes (Scenario C) to 147,900 tonnes (Scenario B); Scenario A generates 65.1% (PV) and 65.6% (BESS) of Scenario B volumes in 2060. Scenario C creates 38.7% and 39.0%, respectively. Temporally, 80.5% of Scenario B PV waste (77,100 tonnes) and 76.2% of BESS waste (39,700 tonnes) materialize between 2045 and 2060. Table 3 disaggregates 2060 Scenario B stocks into the recoverable fractions and hazardous components.

Table 2: Cumulative PV and Lithium-Ion BESS Waste Generation by Scenario, 2035–2060 (tonnes)

	Scenario A (RD)		Scenario B (AT)		Scenario C (CG)	
Year	PV	BESS	PV	BESS	PV	BESS
2035	1,200	800	1,800	1,200	700	500
2045	12,500	8,200	18,700	12,400	7,300	4,800
2050	26,900	18,400	42,300	28,400	15,800	10,900
2055	43,200	26,300	67,400	40,200	25,400	15,600
2060	62,400	34,200	95,800	52,100	37,100	20,300
2060 95% PI	*49.8k–76.9k*	*27.1k–42.5k*	*76.4k–118.2k*	*41.2k–64.9k*	*29.6k–45.8k*	*16.1k–25.3k*

As, showed in Table 2, cumulative waste from both photovoltaic (PV) modules and lithium-ion battery energy storage systems (BESS) rises sharply from 2035 to 2060 across all cases, with PV consistently (specifically in this setting) accounting for the larger share of mass, broadly speaking. Scenario B (AT) is yielding the highest

cumulative volumes by 2060, reaching 95,800 tonnes of PV and 52,100 tonnes of BESS waste (95% prediction intervals of 76.4k–118.2k and 41.2k–64.9k tonnes), followed by Scenario A (RD) at 62,400 tonnes PV and 34,200 tonnes BESS, and Scenario C (CG) at 37,100 tonnes PV and 20,300 tonnes BESS, in real-world scenarios. Along these dimensions, rapid acceleration arises after 2045 in every individual pathway.

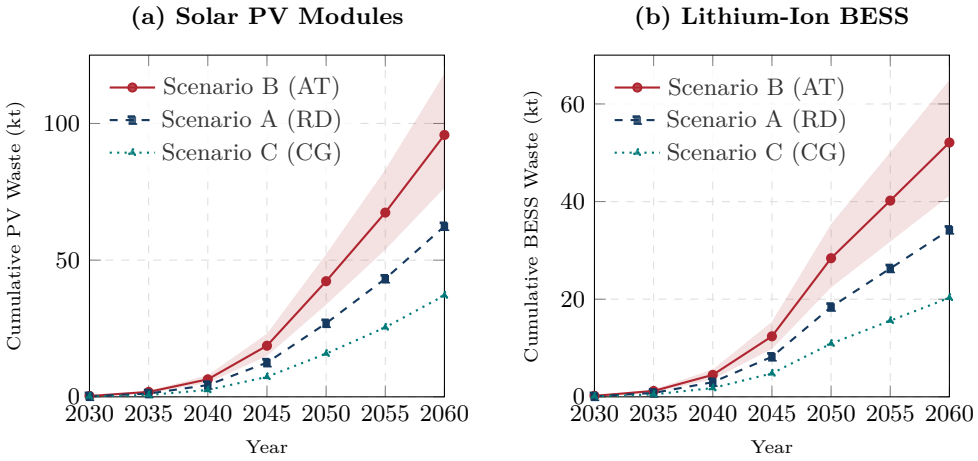


Fig. 2: Cumulative end-of-life waste projections (kilotonnes) in Zimbabwe for (a) solar PV modules and (b) lithium-ion BESS through 2060. Shaded bands denote 95% Monte Carlo prediction intervals for Scenario B ($N = 10{,}000$).

5.2 Deferred Waste Liability Index (DWLI_t) and Capacity Breaches

Across the entire horizon, under Zimbabwe's current status quo (QLATEXz0000q), QLATEXz0001q. In light of this dynamic, to benchmark timing sensitivity under the incremental policy action, QLATEXz0008q is comparing a QLATEXz0009q (a 2,000 t yrQLATEXz0002q hub commissioned in 2033 scaling to a static 5,000 t yrQLATEXz0003q nameplate cap by 2040 at QLATEXz0004q, i.e., 3,500 t yrQLATEXz0005q effective capacity) against the QLATEXz0010q (scaling to 15,000 t yrQLATEXz0006q nameplate by 2045 and 25,000–30,000 t yrQLATEXz0007q by 2050), broadly speaking.

Under the Baseline Pilot Trajectory, $\mathrm{DWLI}_t^{\mathrm{base}}$ remains below 0.30, through 2040; this is demonstrating manageable early-failure flows, broadly speaking, yet concurrent retirement of 2025–2030 utility-scale PV and BESS groups is driving a rapid breach:

Table 3: Cumulative Material Inventory and Recoverable Mass by 2060 under Scenario B

Stream	Material Component	Share (%)	Total Mass (t)	70% Formal Recovery (t)
PV Modules (95,800 t)	Glass cullet	70.0	67,060	46,942
	Aluminium frames	18.0	17,244	12,071
	Polymers / EVA	6.0	5,748	4,024
	Metallurgical / solar silicon	3.5	3,353	2,347
	Copper interconnects	1.5	1,437	1,006
	Trace metals (Ag, Sn–Pb, Cd)[a]	1.0	958	671
BESS (NMC) (52,100 t)	Cathode (Li, Ni, Mn, Co)	27.0	14,067	9,847
	Casing / thermal housing	20.0	10,420	7,294
	Cu / Al current collectors	20.0	10,420	7,294
	Graphite anode	17.0	8,857	6,200
	Electrolyte ($LiPF_6$ / solvents)[b]	12.0	6,252	4,376
	Polymer separator	4.0	2,084	1,459

[a] Includes ≈ 335 t solder lead (0.35% module mass) and ≈ 11.5 t Cd (1.5% CdTe fleet share).

[b] Informal dismantling releases ≈ 45% (∼ 2,813 t) as volatile fluorides and soil leachate.

$\mathrm{DWLI}_t^{\mathrm{base}}$ is crossing 1.0 at $t^* \approx 2042.5$, reaches 1.80 in 2045, and peaks at 3.40 in 2050 ($\dot{W}(2050) \approx 11{,}900\ \mathrm{t\,yr^{-1}}$ against $3{,}500\ \mathrm{t\,yr^{-1}}$ effective capacity), accumulating a preparedness deficit of $\mathcal{D}_{2060} \approx 79{,}400$ tonnes, on the whole. In this broader context, consistent with Corollary 2.1, sustaining $\mathrm{DWLI}_t^{\mathrm{plan}} \leq 0.92 < 1.0$ is needing passing EPR governance before 2030.

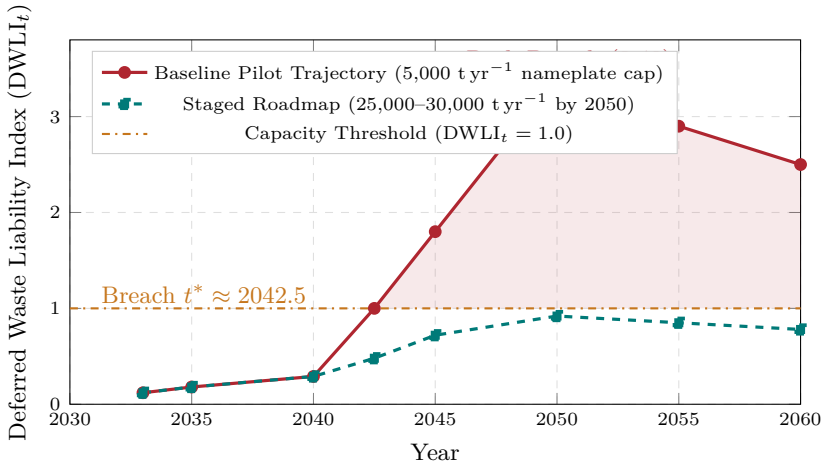


Fig. 3: Deferred Waste Liability Index (DWLI$_t$) trajectories under Scenario B, 2033–2060 ($\phi = 0.70$). Under zero existing capacity, DWLI$_t \to +\infty$; under a frozen 5,000 t yr^{-1} pilot baseline, capacity breaches persist from 2042.5 through 2060.

Figure 3 shows that under one second frozen 5,000 t yr^{-1} baseline pilot capacity, the Deferred Waste Liability Index (DWLI$_t$) remains below the critical threshold (DWLI$_t = 1.0$) through this early 2040s before breaching capacity at $t^* \approx 2042.5$ and increasing sharply to any peak of 3.40 in 2050, after which it intermediates slightly yet remains well above 1.0 (ending at 2.50 in 2060), which is signaling the persistent structural waste backlog, broadly speaking. Within this framework, by contrast, expanding processing capacity to 25,000-30,000 t yr^{-1} under the staged roadmap keeps DWLI$_t$ consistently (specifically in this setting) below the 1.0 threshold across the entire 2033-2060 horizon, peaking at 0.92 in 2050 and declining to 0.78 by 2060, revealing that timely capacity scaling prevents pervasive end-of-life accumulation, on the whole.

5.3 Life Cycle Impacts and Circularity-Weighted Energy Return

Table 4 reports disaggregated and fleet-weighted EoL LCA impacts per tonne of waste. In parallel with this, informal dismantling is producing 3.2 times higher carcinogenic human toxicity for PV modules (driven by Sn–Pb solder and Cd volatilization/leaching during the open burning) and 8.7 times higher carcinogenic human toxicity for NMC lithium-ion batteries (driven by cobalt, nickel, copper, and $LiPF_6$/HF exposure) than formal mechanical and hydrometallurgical recovery, to a significant degree. On the contrary, formal recycling yields net abiotic resource

depletion credits (-0.8 kg Sb-eq t^{-1} mixed; -2.1 kg Sb-eq t^{-1} BESS) by displacing primary silicon, aluminium, copper and cathode-metal sharpening [5, 10], in real-world scenarios.

Table 4: Life Cycle Impacts by End-of-Life Pathway (per tonne retired hardware)

Stream	**Impact Category (Unit)**	**Formal Recycling**	**Informal Dismantling**	**Sanitary Landfill**
PV Modules	Human toxicity, cancer (CTUh)	0.005	0.016 (3.2×)	0.009
	Resource depletion (kg Sb-eq)	−0.10 (credit)	0.15	0.05
BESS (NMC)	Human toxicity, cancer (CTUh)	0.013	0.113 (8.7×)	0.018
	Resource depletion (kg Sb-eq)	−2.10 (credit)	0.58	0.19
Mixed Fleet[a]	Climate change (kg CO_2-eq)	420	680	310
(65% PV / 35% BESS)	Human toxicity, cancer (CTUh)	0.008	0.050	0.012
	Human toxicity, non-cancer (CTUh)	0.042	0.180	0.065
	Freshwater ecotoxicity (CTUe)	12.4	48.2	22.7
	Resource depletion (kg Sb-eq)	−0.80 (credit)	0.30	0.10

[a] Weighted by cumulative Scenario B 2060 mass shares (64.8% PV, 35.2% BESS).

Figure 4 contrasts baseline energy return ($EROI_0 = 12.4$ for PV; $ESOI_0 = 4.2$ for BESS) against CWER; Under Theorem 1, formal recovery satisfies (8) (with minimum doable weighted recovery thresholds $\bar{\eta}_{\min} = 0.28$ for PV and 0.24 for BESS by Corollary 1.2), raising PV CWER by 19.4% (to 14.8) and BESS CWER by 45.2% (to

6.1), in many respects. In opposition, under informal dismantling (Corollary 1.1), non-recovery of silicon and cathode metals coupled with soil/water remediation equivalents depresses CWER to 11.2 for PV (−9.7%) and 3.8 for BESS (−9.5%), in many respects. On a unit-mass basis, formalizing EoL recovery preserves net embodied energy of 3.6 MWh t^{-1} for PV and 8.4 MWh t^{-1} for BESS relative to informal disposal; across Scenario B cumulative 2060 stocks, theoretical maximum savings total 782.5 GWh (344.9 GWh PV; 437.6 GWh BESS), creating 547.8 GWh of realized energy savings at $\phi = 0.70$.

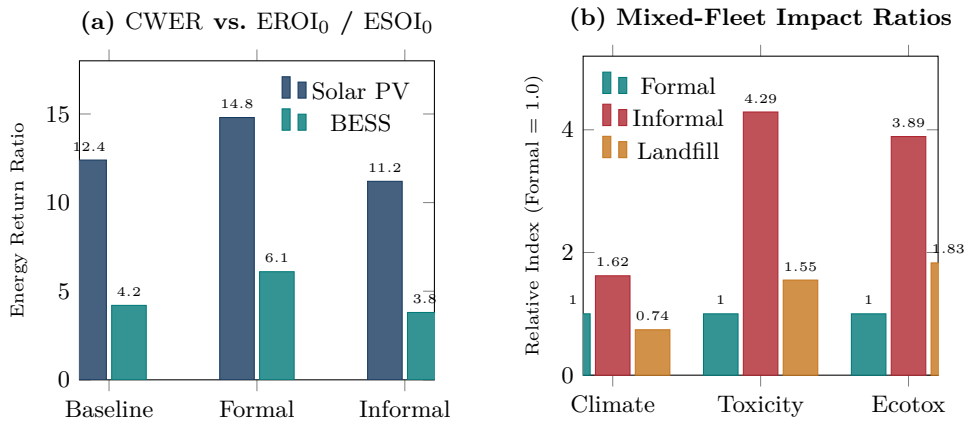


Fig. 4: Comparison of (a) Circularity-Weighted Energy Return (CWER) across pathways and (b) normalized mixed-fleet LCA impact ratios relative to formal recycling (Toxicity = non-cancer CTUh).

5.4 Local Case Studies for Operational and Spatial Robustness

To test robustness across the mixed deployment scales, operational profiles, and reverse-logistics geographies, Table 5 appraises three representative Zimbabwean archetypes:

1. **Case Study 1 — Matabeleland/Midlands Utility-Scale IPP Corridor (100 MWp PV + 40 MW/160 MWh BESS):** Bulk containerized decommissioning is decreasing reverse-logistics costs to USD 380–520 tQLATEXz0000q via rail links to Bulawayo and Durban, reaching high formal encapsulate (QLATEXz0001q) and raising BESS QLATEXz0002q to QLATEXz0003q supplied decommissioning bonds are particularly ring-fenced in ZERA power purchase

agreements, in real-world scenarios. In light of this dynamic, high-irradiance ground-mount plant along the Bulawayo–Gweru transmission corridor.

2. **Case Study 2 — Harare/Msasa and Great Dyke C&I/Mining Microgrid (2 MWp PV + 4 MWh BESS):** Intensive depth-of-discharge compresses BESS mean lifetime ($\bar{L}_{\mathrm{BESS}} = 9.0$ years), doubling replacement frequency and raising present-value EoL reserve needs; mandatory distributor take-back agreements are generating $\phi \approx 0.75$ and BESS CWER = 5.8, broadly speaking; captive commercial and mining hybrid systems cycling daily to offset diesel backup and grid curtailment, in real-world scenarios.
3. **Case Study 3 — Mashonaland/Masvingo Rural SHS and Mini-Grid Cluster (5 MWp PV + 10 MWh BESS aggregate across ∼3,200 units):** Spatially dispersed household systems suffer severe reverse-logistics penalties (USD 1,150–1,600 t^{-1}) and high informal leakage risks ($\phi \approx 0.25$ absent intervention). In this broader context, without a point-of-sale battery deposit-refund and certified informal collector cooperatives, informal dismantling depresses BESS CWER to 3.6 and concentrates direct and fluoride contamination around rural service centres.

5.5 Parametric Sensitivity and Robustness Analysis

Figure 5 quantifies one-at-a-time elasticity of Scenario B 2060 combined cumulative waste (147,900 t baseline) and actuarial charges τ_i, across key parametric perturbations, to a significant degree. Mean module lifetime ($\bar{L}_{\mathrm{PV}} \pm 4$ yr) is exerting the largest use on 2060 cumulative waste (-14.2% to $+16.8\%$), followed by group mass-intensity light-weighting rate ($\pm 0.4\%\,\mathrm{yr}^{-1}$; $\pm 9.1\%$), Weibull shape ($\alpha_i \pm 0.5$; $\pm 6.4\%$), and customs leakage ($\rho_{i,t} \in [0.02, 0.15]$; $\pm 4.3\%$), to a significant degree. In this broader context, crucially, across the entire 95% multivariate Monte Carlo envelope, the Scenario B capacity-breach year t^* shifts only between 2041.2 and 2044.1, proving that the pre-2030 policy enactment window (Corollary 2.1) is structurally invariant to tenable parametric uncertainty.

max width=

Table 5: Local Case-Study Validation Across Zimbabwean Deployment Archetypes

Attribute	**Case 1: Utility IPP**	**Case 2: C&I / Mining**	**Case 3: Rural SHS Cluster**
Location archetype	Bulawayo–Gweru corridor	Harare / Great Dyke	Mashonaland / Masvingo
Installed scale	100 MWp PV / 160 MWh	2 MWp PV / 4 MWh	5 MWp PV / 10 MWh (agg.)
BESS mean lifetime $\bar{L}$	12.0 yr (grid-managed)	9.0 yr (deep cycling)	8.5 yr (uncontrolled DoD)
Lifecycle waste mass	7,560 t (PV+BESS)	158 t (2 BESS cycles)	395 t (dispersed)
Reverse-logistics cost	USD 380–520 t^{-1}	USD 620–850 t^{-1}	USD 1,150–1,600 t^{-1}
Unmitigated capture ϕ	0.65 (site stockpiling)	0.45 (scrap leakage)	0.15–0.25 (informal)
BESS CWER (Mitigated / Unmit.)	6.4 / 4.0	5.8 / 3.9	5.3 / 3.6
Primary governance lever	ZERA PPA decomm. bond	Distributor take-back	Deposit-refund + co-ops

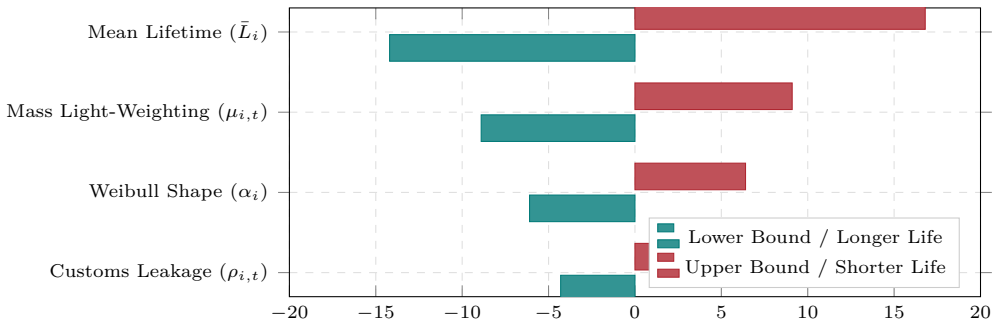


Fig. 5: Tornado sensitivity analysis of Scenario B 2060 combined cumulative waste (baseline 147,900 t) across key MFA parameter perturbations.

6 Discussion and Policy Implications

6.1 Mitigating Deferred Liabilities and Phased Infrastructure Scale-Up

The DWLI_t results expose an acute intertemporal vulnerability widespread to import-dependent solar transitions: resolving near-term power deficits creates an unfunded environmental blame maturing promptly beyond current 2040 energy-planning horizons, on the whole; in fact, under total informal dismantling of Scenario B stocks through 2060, cumulative hazardous releases are reaching roughly 335 tonnes of solder lead, 11.5 tonnes of cadmium, and 2,813 tonnes of unpredictable or leachable fluorinated electrolyte compounds, alongside everywhere cobalt and nickel contamination, in actual application.

Reaching the 70% formal recovery target under Scenario B is needing expanding effective processing capacity from zero to 25,000–30,000 $\mathrm{t\,yr^{-1}}$ nameplate (17,500–21,000 $\mathrm{t\,yr^{-1}}$ effective) by 2050. Along these dimensions, international benchmarks place capital expenditure at USD 8–12 million for a 5,000 $\mathrm{t\,yr^{-1}}$ mechanical PV delamination line and USD 15–25 million for an equal hydrometallurgical battery facility [5, 10], with reverse logistics adding 40–60% to total lifecycle system costs. Table 6 details a staged 2026–2050 infrastructure and regulatory roadmap aligned with Corollary 2.1.

6.2 Three-Tiered Import-Anchored EPR Architecture

Standard OECD and South African EPR models depend on domestic manufacturers and solid post-market enforcement [6]. In Zimbabwe, where hardware is 100% imported, presently under NREP duty-free incentives [18]—regulatory apply is strongest at customs ports of entry and weakest across the scattered retail outlets. In parallel with this, preserving duty-free customs status for clean generation while internalizing EoL costs needs a ring-fenced, three-tiered EPR architecture:

Tier 1: Customs-Anchored Sinking-Fund Levy.

Replace ad hoc municipal tipping burdens with a dedicated, actuarially optimized environmental fee (2–4% of CIF import value, phased over five years) collected by ZIMRA under HS 8541.40 and HS 8507.60 and ring-fenced within an independently audited Sovereign Circularity Fund jointly dictated by regulators, importers, recyclers and civil society, in actual application.

Table 6: Phased Infrastructure Roadmap and Institutional Milestones (2026–2050)

Phase	Target Capacity	Physical Infrastructure	Policy & Governance Action
2026–2030	Regulatory base	Regional testing lab; municipal drop-off pilots	Enact import EPR levy; establish independent PRO fund; ban landfilling
2030–2035	2,000 $\mathrm{t\,yr^{-1}}$	Harare & Bulawayo hubs; battery diagnostic & second-life lab	Certify informal collectors; launch BESS deposit-refund (USD 5–10)
2035–2040	5,000 $\mathrm{t\,yr^{-1}}$	Provincial consolidation depots; mechanical PV delamination line	Ratify SADC Basel transboundary corridors for black-mass export
2040–2045	15,000 $\mathrm{t\,yr^{-1}}$	Capacity tripling; thermal/chemical Si & Ag recovery	Enforce 50–70% importer take-back quotas; audit PRO solvency
2045–2050	25,000–30,000 $\mathrm{t\,yr^{-1}}$	Full-scale regional circularity hub	Mandate design-for-recycling procurement standards on imports

Tier 2: Distributor Take-Back and Deposit-Refund.
Importers and ZERA-registered IPPs were licensed by need to finance urban take-back networks with increasing collection quotas (20% by 2030 to 70% by 2045), strengthened by a USD 5–10 point-of-sale deposit-refund on residential battery packs to curb rural and peri-urban dumping (Case Study 3), on the whole.

Tier 3: Formal–Informal Sector Integration.
Rather than criminalizing informal scrap dealers, which depresses collection rates [24]—PRO revenues should fund occupational certification, protective equipment, and guaranteed off-take tariffs for intact modules and undismantled battery packs delivered to certified consolidation hubs [15], on the whole.

6.3 Quantitative Assessment of SADC Regional Hub-and-Spoke Mitigation

Employing Proposition 4 thoroughly is appraising regional versus domestic battery recycling strategies. In light of this dynamic, applying regional techno-economic factors at real discount rate $r = 0.08$ over a 15-year plant horizon (CRF = 0.1168): a domestic hydrometallurgical plant (K_{dom} = USD 2.34M $\mathrm{yr^{-1}}$ from USD 20M capex; v_{dom} = USD 1,200 $\mathrm{t^{-1}}$) versus domestic discharging/black-mass pre-processing

(K_{pre} = USD 0.58M yr^{-1} from USD 5M capex; v_{pre} = USD 450 t^{-1}) with black-mass concentration $\theta = 0.45$, rail/road freight to South Africa c_{trans} = USD 280 t^{-1}, and regional hydrometallurgical gate fee v_{reg} = USD 1,650 t^{-1} produces a scale threshold of

$$W^*_{\text{hydro}} = \frac{2{,}336{,}591 - 584{,}148}{450 + 0.45(280 + 1{,}650) - 1{,}200} = 14{,}789 \text{ t yr}^{-1}.$$

Because, Zimbabwe's annual Scenario B BESS retirement flow is remaining below 5,500 t yr^{-1}, through 2055 (well below W^*_{hydro}), domestic mechanical PV delamination paired with domestic BESS black-mass pre-processing and SADC regional hydrometallurgical sharpening in South Africa's NEMWA-regulated ecosystem [6] saves USD 1.1–1.5 million annually in avoided fixed-capital underutilization, in actual application. Under these conditions, effectuating this corridor requires harmonizing SADC waste classification codes and starting sped up Basel Convention prior-informed-consent (PIC) transit protocols before 2040, in real-world scenarios.

6.4 Internalizing Circularity into Stochastic Mean-CVaR Energy Planning

Capital cost and drought-risk hedging are sharpened by National Mean-CVaR generation expansion models while treating EoL decommissioning as a zero-cost externality [21, 26], on the whole. Taken together, evaluating Proposition 3 at $r = 0.08$ and $\phi^{\text{target}} = 0.70$ is generating exact Weibull Laplace changes $\mathcal{L}\{f_{\text{PV}}\}(0.08) = 0.1877$ ($\bar{L}_{\text{PV}} = 25$ yr, $\alpha_{\text{PV}} = 2.5$, $\beta_{\text{PV}} = 28.18$) and $\mathcal{L}\{f_{\text{BESS}}\}(0.08) = 0.4361$ ($\bar{L}_{\text{BESS}} = 11$ yr, $\alpha_{\text{BESS}} = 3.0$, $\beta_{\text{BESS}} = 12.32$), to a significant degree.

For PV modules ($\mu_{\text{PV}} = 0.062$ t kW^{-1}) with net EoL treatment and logistics cost $c^{\text{EoL}}_{\text{PV}} \in [1{,}850, 3{,}050]$ USD t^{-1}, (10) is producing τ_{PV} = USD 15.1–24.9 kW^{-1} (approx. USD 15–25 kW^{-1}), in real-world scenarios; across both technologies, internalizing τ_i adds only 2–3% to upfront installed capital cost [13], avoiding distortion of clean-energy competitiveness while excluding unfunded municipal waste debt, on the whole. In parallel with this, for BESS packs ($\mu_{\text{BESS}} = 0.0085$ t kWh^{-1}) with net hazardous EoL cost $c^{\text{EoL}}_{\text{BESS}} \in [4{,}000, 6{,}900]$ USD t^{-1}, the single-cohort levy is $\tau^{(1)}_{\text{BESS}}$ = USD 10.4–17.9 kWh^{-1} (rising to USD 14.0–24.2 kWh^{-1} for containerized balance-of-plant frameworks at 11.5 t MWh^{-1}, and USD 19–33 kWh^{-1} when reserving for a second battery replacement cohort over a 25-year PV project horizon).

7 Conclusions

A generalizable, statistically triangulated MFA–LCA and EPR optimization framework for import-dependent emerging economies was devised by that article and substantiated it employing Zimbabwean national data and three local deployment case studies. Without proactive intervention, 57,400–147,900 are yielded by Zimbabwe's solar PV and BESS expansion tonnes of cumulative EoL waste by 2060 (95,800 tonnes PV and 52,100 tonnes BESS under Accelerated Transition). Applying the regularized DWLI_t metric and Proposition 2, we reveal that an acute capacity deficit will materialize between 2042 and 2050 unless binding EPR legislation and staged infrastructure investments are passed before 2030. Within this framework, informal dismantling degrades net energy return and multiplies carcinogenic human toxicity up to 8.7-fold. Thermodynamically coherent CWER analysis (Theorem 1) is corroborating that formal recovery augments net system energy return by 19.4% for PV and 45.2% for BESS, preserving 547.8 GWh of embodied energy at 70% collection.

A three-tiered, customs-anchored EPR system capitalized through the actuarially fair sinking-fund charges (USD 15–25 kW^{-1} for PV; USD 10.4–17.9 kWh^{-1} per BESS cohort), paired with informal-collector certification and SADC regional hydrometallurgical cooperation (strictly best below 14,789 $\mathrm{t\,yr}^{-1}$), is supplying a fiscally workable circularity pathway, to a significant degree; and thus, post-2040 capacity extrapolations, reliance on international material-intensity benchmarks for emerging sodium-ion and perovskite-tandem chemistries, and capital-cost uncertainties for regional plants are encompassed by key shortcomings, on the whole. Possible efforts ought to integrate satellite remote sensing to sharpen distributed rooftop inventories and expand national MFA accounting to power inverters and lead-acid storage fleets.

Data Availability

Stated separately, Data obtain from publicly available literature, reports, and secondary sources; supporting materials are, in effect, available from the corresponding author upon reasonable request, broadly speaking.

Ethics Statement

To be precise, Not applicable; no human participants, personal data, animals, or human-subject tests were encompassed, on the whole.

Consent to Participate

Not applicable; the study entailed no human participants.

Consent for Publication

Most markedly, not applicable; no identifiable individual-level data are reliably encompassed.

Funding

Remarkably, the current study received no particular grant from public, commercial, or not-for-profit funding agencies, in actual application.

Competing Interests

No competing interests are, by design, declared by the author(s).

Author Contributions

The author(s) conceived and designed the study, built the modelling framework, analysed and construed findings, and drafted and revised the manuscript, approving the final version.

Declaration of Generative AI and AI-Assisted Technologies

Generative AI tools were applied solely to help with language editing and drafting polish; the author(s) validated all content and take full responsibility for this manuscript, in real-world scenarios.

Code Availability

Computational protocols and analytical code are, strictly speaking, available from the corresponding author upon reasonable request, in many respects.

Acknowledgements

None to declare.

References

[1] Badza, K., Sawadogo, M., & Soro, Y. M. (2024). Environmental impacts of a stand-alone photovoltaic system in sub-Saharan Africa: A case study in Burkina Faso. *Heliyon*, 10(19), e38954.

[2] Baldé, C. P., Kuehr, R., Yamamoto, T., McDonald, R., D'Angelo, E., Althaf, S., Bel, G., Deubzer, O., Fernandez-Cubillo, E., Forti, V., Gray, V., Herat, S., Honda, S., Iattoni, G., Khetriwal, D. S., Luda di Cortemiglia, V., Lobuntsova,

Y., Nnorom, I., Pralat, N., & Wagner, M. (2024). *The Global E-waste Monitor 2024*. Geneva/Bonn: International Telecommunication Union (ITU) and United Nations Institute for Training and Research (UNITAR).

[3] Barnhart, C. J., & Benson, S. M. (2013). On the importance of reducing the energetic and material demands of electrical energy storage. *Energy & Environmental Science*, 6(4), 1083–1092.

[4] Chowdhury, M. S., Rahman, K. S., Chowdhury, T., Nuthammachot, N., Techato, K., Akhtaruzzaman, M., Tiong, S. K., Sopian, K., & Amin, N. (2020). An overview of solar photovoltaic panels' end-of-life material recycling. *Energy Strategy Reviews*, 27, 100431.

[5] Ciez, R. E., & Whitacre, J. F. (2019). Examining different recycling processes for lithium-ion batteries. *Nature Sustainability*, 2(2), 148–156.

[6] Department of Forestry, Fisheries and the Environment [DFFE]. (2020). *Regulations Regarding Extended Producer Responsibility (Government Notice No. 1184, National Environmental Management: Waste Act, 2008 [Act No. 59 of 2008]).* Pretoria: Republic of South Africa.

[7] Domínguez, A., & Geyer, R. (2017). Photovoltaic waste assessment in Mexico. *Resources, Conservation and Recycling*, 127, 29–41.

[8] Farrell, C. C., Osman, A. I., Doherty, R., Saad, M., Zhang, X., Murphy, A., Harrison, J., Vennard, A. S. M., Kumaravel, V., Al-Muhtaseb, A. H., & Rooney, D. W. (2020). Technical challenges and opportunities in realising a circular economy for waste photovoltaic modules. *Renewable and Sustainable Energy Reviews*, 128, 109911.

[9] Harper, G., Sommerville, R., Kendrick, E., Driscoll, L., Slater, P., Stolkin, R., Walton, A., Christensen, P., Heidrich, O., Lambert, S., Abbott, A., Ryder, K., Gaines, L., & Anderson, P. (2019). Recycling lithium-ion batteries from electric vehicles. *Nature*, 575(7781), 75–86.

[10] Heath, G. A., Silverman, T. J., Kempe, M., Deceglie, M., Ravikumar, D., Remo, T., Cui, H., Sinha, P., Libby, C., Shaw, S., Komoto, K., Wambach, K., Butler, E., Barnes, T., & Wade, A. (2020). Research and development priorities for silicon photovoltaic module recycling to support a circular economy. *Nature Energy*,

5(7), 502–510.

[11] Hou, L. (2026). Differences in global multi-regional photovoltaic expansion from 1980 to 2050: A focus on demand, recycling, and local-supply exposure for critical minerals. *Journal of Environmental Management*, 417, 130892.

[12] International Energy Agency [IEA]. (2024). *World Energy Outlook 2024*. Paris: IEA Publications.

[13] International Renewable Energy Agency [IRENA]. (2024). *Renewable Power Generation Costs in 2024*. Abu Dhabi: IRENA.

[14] Jorio, M., Amaral, A., & Ferreira, P. (2026). Dynamic and probabilistic material flow analysis for circular economy strategies in the photovoltaic sector. *Environment, Development and Sustainability*. https://doi.org/10.1007/s10668-026-07730-6

[15] Kumba, H., Makepa, D. C., Charamba, A. N., & Olanrewaju, O. A. (2024). Towards circular economy: Integrating waste management for renewable energy optimization in Zimbabwe. *Sustainability*, 16(12), 5014.

[16] Latunussa, C. E. L., Ardente, F., Blengini, G. A., & Mancini, L. (2016). Life cycle assessment of an innovative recycling process for crystalline silicon photovoltaic panels. *Solar Energy Materials and Solar Cells*, 156, 101–111.

[17] Mahmoudi, S., Huda, N., Alavi, Z., & Behnia, M. (2019). End-of-life photovoltaic modules: A systematic quantitative literature review. *Resources, Conservation and Recycling*, 146, 1–16.

[18] Ministry of Energy and Power Development [MEPD]. (2019). *National Renewable Energy Policy*. Harare: Government of Zimbabwe.

[19] Nnorom, I. C., & Osibanjo, O. (2008). Overview of electronic waste (e-waste) management practices and legislations, and their poor applications in the developing countries. *Resources, Conservation and Recycling*, 52(6), 843–858.

[20] Raugei, M., Fullana-i-Palmer, P., & Fthenakis, V. (2012). The energy return on energy investment (EROI) of photovoltaics: Methodology and comparisons with fossil fuel life cycles. *Energy Policy*, 45, 576–582.

[21] Rockafellar, R. T., & Uryasev, S. (2000). Optimization of conditional value-at-risk. *Journal of Risk*, 2(3), 21–41.

[22] United Nations Economic Commission for Europe [UNECE]. (2021). *Life Cycle Assessment of Electricity Generation Options*. Geneva: United Nations.

[23] Weckend, S., Wade, A., & Heath, G. (2016). *End-of-Life Management: Solar Photovoltaic Panels*. Abu Dhabi/Paris: IRENA and IEA-PVPS.

[24] Wilson, D. C., Velis, C., & Cheeseman, C. (2006). Role of informal sector recycling in waste management in developing countries. *Habitat International*, 30(4), 797–808.

[25] Xu, Y., Li, J., Tan, Q., Peters, A. L., & Yang, C. (2018). Global status of recycling waste solar panels: A review. *Waste Management*, 75, 450–458.

[26] Zimbabwe Energy Regulatory Authority [ZERA]. (2025). *2024 Annual Report*. Harare: ZERA.

A Notation and Definitions

@>p0.32 >p0.64@

Symbol	Definition
$\hat{I}_{i,t},\ w_{i,t}$	Minimum-variance triangulated annual capacity addition and best weight
$\rho_{i,t},\ \mu_{i,\tau}$	Informal/re-export leakage fraction and batch mass intensity ($\mathrm{t\,MW^{-1}}$ or $\mathrm{t\,MWh^{-1}}$)
$F_i(\Delta;\alpha_i,\beta_i)$	Weibull cumulative retirement distribution with shape α_i and scale β_i
$\dot{W}_{i,t},\ W_{i,T}$	Annual EoL waste flow ($\mathrm{t\,yr^{-1}}$) and cumulative waste, through the year T (t)
$C_{i,t},\ \phi_i$	Installed recycling capacity ($\mathrm{t\,yr^{-1}}$) and attainable recovery efficiency

DWLI_t, $\mathcal{D}_T$ Deferred Waste Liability Index and Cumulative Preparedness Deficit (t)

Δ_{inst}, κ Institutional-to-commissioning lag (yr) and linear capacity ramp rate ($\mathrm{t\,yr^{-2}}$)

E_{out}, E_{in} Lifetime electricity output and manufacturing/BoS embodied energy

E_{EoL}, E_{rem} EoL processing energy investment and environmental remediation energy penalty

M_m^{EoL}, e_m, η_m Mass, unit primary embodied energy, and recovery efficiency of material m

EROI_0, CWER, $\bar{\eta}_{\mathrm{min}}$ Baseline energy return, Circularity-Weighted Energy Return, and viability bound

τ_i, r, c_i^{EoL} Upfront EPR sinking-fund charge, real discount rate, and net unit EoL cost

W^*_{hydro}, θ Regional hydrometallurgical scale threshold ($\mathrm{t\,yr^{-1}}$) and black-mass share

---

Supplementary Files

This is a list of supplementary files associated with this preprint. Click to download.

- Manuscriptwithauthordetails.zip